Amino Acids (2010) 39:661–670
DOI 10.1007/s00726-010-0487-5

ORIGINAL ARTICLE

γ-Glutamyl 16-diaminopropane derivative of vasoactive intestinal peptide: a potent anti-oxidative agent for human epidermoid cancer cells

Paola Stiuso · Gaia Giuberti · Angela Lombardi · Alessandra Dicitore · Vittorio Limongelli · Maria Cartenì · Alberto Abbruzzese · Michele Caraglia

Received: 25 September 2009 / Accepted: 15 January 2010 / Published online: 10 February 2010

Abstract We previously demonstrated that the γ-glutamyl 16 amine derivative of vasoactive intestinal peptide (VIP) acts as structural VIP agonist with affinity and potency higher than VIP. Herein, we have evaluated the effects of VIP and γ-Gln16-diaminopropane derivative of VIP (VIP-DAP3) on the proliferation and protection from oxidative stress induced by hydrogen peroxide (H_2O_2) on epidermoid carcinoma cell lines. We have found that 10^{-11} M VIP-DAP3 completely antagonized the inhibition induced by H_2O_2 on both cell proliferation and S-phase distribution while these effects were only partially antagonized by equimolar concentrations of VIP. Moreover, both oxidative stress and intracellular lipid oxidation induced by H_2O_2 were reduced by VIP and completely antagonized by VIP-DAP3. Thereafter, we have found that H_2O_2 increased p38 kinase activity and both HSP70 and HSP27 expression. VIP and VIP-DAP3 again antagonized these effects partially or totally, respectively. H_2O_2 reduced the activity of extracellular signal-regulated kinases Erk-1/2 and Akt, signalling proteins involved in proliferation/survival pathways. Again VIP restored the activity of both kinases while VIP-DAP3 caused indeed an increase of their activity as compared to untreated cells. These data suggest that VIP-DAP3 has a stronger anti-oxidative activity as compared to VIP likely based on its super-agonistic binding on the putative receptor.

Keywords Akt · Extracellular signal-regulated kinases Erk-1/2 · p38 kinase · Oxidative stress · Proliferation · Vasoactive intestinal peptide (VIP) · γ-Glutamyl 16 amine vasoactive intestinal peptide (VIP-DAP3)

Abbreviations

DMEM	Dulbecco's modified Eagle medium
RPMI	Roswell Park Memorial Institute medium
KB	Human oropharyngeal epidermoid carcinoma
H1355	Lung epidermoid NSCLC
Dap	1,3-Diaminopropane
NO	Nitric oxide
PACAP	Pituitary adenylate cyclase-activating peptide
Pt	Put rescine
Spd	Spermidine
Spm	Spermine
TGase	Transglutaminase
VIP	Vasoactive intestinal peptide
VPAC1	V IP/PACAP1 receptor
VPAC2	V IP/PACAP2 receptor
VIP-DAP	γ-Glutamyl l6-diaminopropane derivative of vasoactive intestinal peptide
RP-HPLC	Reverse-phase HPLC
SOD	Superoxide dismutase
GPX	Glutathione peroxidase
p38 MAPK	p38 mitogen-activated protein kinases

P. Stiuso · G. Giuberti · A. Lombardi · A. Dicitore · A. Abbruzzese · M. Caraglia (✉)
Department of Biochemistry and Biophysics, Second University of Naples, Via Costantinopoli 16, 80138 Naples, Italy
e-mail: Michele.caraglia@unina2.it; Michele.caraglia@alice.it

V. Limongelli
Department of Pharmaceutical and Toxicological Chemistry, University of Naples Federico II, Via D. Montesano 49, 80131 Naples, Italy

M. Cartenì
Department of Experimental Medicine, Second University of Naples, Via Costantinopoli 16, 80138 Naples, Italy

SAPK/JNK	Stress-activated protein kinase/c-Jun NH2-terminal kinase
AKT	Serine/threonine kinase
GSK-3	Glycogen synthase kinase
HE	Hydroethidine

Introduction

Vasoactive intestinal peptide (VIP) is a 28 amino acid long peptide and is a member of the secretin–glucagon family of regulatory peptides involved in the modulation of numerous biological functions (Sherwood et al. 2000). VIP is a potent relaxant of human airway smooth muscle and pulmonary blood vessels (Matsuzaki et al. 1980; Saga and Said 1984; Groneberg et al. 2001), inhibits the release of macromolecules from secreting glands (Coles et al. 1981; Martin and Shuttleworth 1996), functions as neurotransmitter of the nonadrenergic–noncholinergic inhibitory nervous system (Cameron et al. 1983; Cooke 2000; Nussdorfer et al. 2000), produces anti-inflammatory effects (Said 1991; Delgado et al. 2002), modulates T-cell and B-cell proliferation (Ishioka et al. 1992; De Maria et al. 2002), and inhibits human natural killer cell activity (Holtmann et al. 1995). Moreover, it has been shown to promote the growth and differentiation of a variety of cells in tissue and organ cultures (Koh and Waschek 2000). In cultured retinal cells, VIP is the one most effective stimulator of the cyclic adenosine monophosphate (cAMP)-signalling pathway among a long list of neurotransmitters and modulators. Actually, VIP attenuates cell death caused by the oxidative stress induced by glutamate in cultured rat retinal neurons through a cAMP/protein kinase A-dependent mechanism (Shoge et al. 1998).

VIP may be an autocrine trophic factor that protects corneal endothelial (CE) cells from H_2O_2 in normal aqueous humour and possibly also from other oxidative insults (Koh and Waschek 2000). At least two different G-protein-coupled receptors, named VPAC1 and VPAC2, mediate these actions (Gourlet et al. 1996; Nicole et al. 2000). Robberecht et al. demonstrated the unexpected importance of Gln16 in the central region of the secretin family peptides for its interaction with the receptor N-terminal domain (De Maria et al. 2002). On the basis of this finding, through tissue transglutaminase (TGase) enzyme, primary structure of VIP was modified by addition of several amines at the level of the Gln16 γ-carboxyamide group in order to investigate the effect on VPAC receptor activity, both in rats and humans (Onoue et al. 2004; De Maria et al. 2002). Three polyaminated VIP derivatives were demonstrated to act as VIP agonists with an affinity and a potency on VPAC receptors higher (VIP-DAP3) or lower than VIP [VIP-spermidine (Spd) and VIP spermine (Spm)]. Polyamine carbon chain length and positive charge have a relevance on receptor activation as demonstrated by experiments on murine macrophage J774 in which VIP adducts modulate the in vivo iNOS activity at transcriptional level of (Holtmann et al. 1995; Gourlet et al. 1996; Shoge et al. 1998; Koh and Waschek 2000; De Maria et al. 2002). The IC_{50} and EC_{50} values from binding experiments with human and rat VPAC1 and VPAC2 receptors indicate that VIP-DAP3 has higher affinity and potency than VIP (De Maria et al. 2002; Caraglia et al. 2006; Caraglia et al. 2008). We have investigated the structural features of VIP and VIP-DAP3 in solution by limited proteolysis experiments. VIP-DAP3 appears to be more resistant to proteolytic attack by trypsin, indicating that the derivatization in position 16 stabilizes its structure. Moreover, the analysis of the mass spectra of either VIP or VIP-DAP3 supports the evidence that the derivatization also protects Met17 residue from oxidation (Caraglia et al. 2006).

Oxidative stress is a phenomenon that induces various health alterations and diseases by increased oxidation of biologically important molecules in vivo. Oxidation reactions by reactive oxygen species (ROS) are considered a trigger of the oxidative stress. Several enzymes such as superoxide dismutase (SOD), glutathione peroxidase (GPX) and catalase serve as protective anti-oxidants against oxidative stress (Inanami et al. 1999). It is widely reported that p38 MAPK, MAP kinase (MAPK) leading to apoptosis, is activated by treatment with H_2O_2, but its activation is independent from the increase of Ca^{2+} (Kuwabara et al. 2008). In fact, ROS induce two signalling pathways, an increase of $(Ca^{2+})_i$ and subsequent activation of SAPK/JNK, and the release of cytochrome *c* followed by the activation of p38 MAPK leading to apoptotic cell death (Niwa et al. 2003; Xia et al. 1995). On the other hand, ERK (extracellular signal-regulated kinases), members of proliferative MAPK family, and PKB (protein kinase B, Akt) are known as kinases leading to cell survival (Inanami et al. 1999; Xia et al. 1995). Transient ischaemia induces the activation of both SAPK/JNK and p38 MAPK leading to apoptosis and ERK leading to survival, suggesting that oxidative stress induces both death and survival signalling pathways even in vivo (Tsuji et al. 2000). Our group has recently demonstrated that pre-fibrillar amyloid aggregates (PFAs) increases intracellular ROS and induces apoptosis in neuroblastoma cells (Sirangelo et al. 2009). This effect was paralleled by a time-dependent decrease of p38 kinase activity and HSP-70 expression and a reduction of the survival kinase Akt activity. On the other hand, PFAs induce an early and transitory increase of both ras and rac activities, the latter being involved in the

triggering of intracellular ROS leading to apoptosis occurrence.

In this study, we have investigated VIP and VIP-DAP3 anti-oxidative effects evaluating proliferation and cell-cycle perturbation, intracellular ROS levels and both stress-activated and survival pathway modulation in human epidermoid carcinoma oropharyngeal KB and non-small cell lung cancer (NSCLC) H1355 cell lines.

Materials and methods

Materials

DMEM, BSA and FBS were purchased from Flow Laboratories (Milan, Italy). Tissue culture plasticware was purchased from Becton-Dickinson (Lincoln Park, NJ). VIP was a gift of Sigma-Aldrich (St. Louis, MO). Hydrogen peroxide (H_2O_2) 1 M stock solution was prepared immediately before use. Propidium iodide (PI) was purchased from Applichem (Darmstadt, Germany). Hydroethydine (HE) was purchased from Invitrogen srl (Milan, Italy). Erk-1/2 MAb C-14, rabbit anti-p38(C-20), anti-mouse pp38 (D-8) and JNK1 Mab (F-3) were purchased from Santa Cruz Biotechnology (Santa Cruz, CA). Phospho-p44/42 MAPK MAb, anti-Akt Mab, rabbit anti-pGSK-3α/β and the relative activity-Akt evaluation kit were purchased from Cell Signalling Technology (Beverly, MA). Anti-Heat Shock Protein 70 (Universal) MAb (5A5) and Anti-Heat Shock Protein 27 MAb (G3.1) were purchased from Alexis Biochemicals (Lausen, SW). Anti-α-tubulin MAb (clone Ab-1) was purchased from Oncogene Research Products (Boston, MA, USA). 2-Thiobarbituric acid (TBA), malondialdehyde-bis-(dimethylacetal)-1,1,3,3-tetramethoxypropane (MDA) and 1,3-diaminopropane were purchased from Sigma Chemical Co. (St. Louis, MO, USA). For the production of VIP-DAP3, we have used tissue TGase provided by Sigma (Milan, Italy).

TGase-catalysed synthesis of VIP-DAP3

VIP-DAP3 was obtained by incubating for 12 h in a final volume of 200 µl at 37°C. 50 µg of native VIP with TGase in 125 mM Tris–HCl buffer, pH 8.0, containing 10 mM dithiothreitol, 2.5 mM $CaCl_2$, 0.2 mM DAP, and 6.7 mU TGase were added at the start of incubation, and the same amount of enzyme was added after 6 h. A control sample incubated in the absence of TGase was assessed simultaneously. At the end of the incubation, the reaction mixtures were centrifuged at 12,000*g* for 10 min, and the resulting supernatants were used to purify the VIP-DAP3 by reverse-phase high-performance liquid chromatography (RP-HPLC) as reported in our previous paper (Caraglia et al. 2008).

Cell culture

The human oropharyngeal epidermoid carcinoma KB and the lung epidermoid NSCLC H1355 cell lines were obtained from the American Type Tissue Culture Collection (Rockville, MD) and were grown in DMEM and RPMI, respectively, supplemented with heat-inactivated 10% FBS, 20 mM HEPES, 100 U/ml penicillin, 100 µg/ml streptomycin, 1% L-glutamine and 1% sodium pyruvate. The cells were grown in a humidified atmosphere of 95% air–5% CO_2 at 37°C.

Proliferation assays

For cell proliferation experiments on KB and H1355 cells, 1.0×10^6 control or treated cells were seeded in 100 mm plates in 6 ml of medium and incubated at 37°C. 10^{-10} and 10^{-11} M concentrations of VIP or VIP-DAP3 were added for 12 and 24 h after seeding. At the selected times and concentrations, the cell number was determined with a haemocytometric counter.

Western blot analysis

KB cells were grown for 24 h with VIP or VIP-DAP3 at 37°C, as described above. For cell extract preparation, the cells were washed twice with ice-cold PBS/BSA, scraped, and centrifuged for 30 min at 4°C in 1 ml of lysis buffer (1% Triton, 0.5% sodium deoxycholate, 0.1 M NaCl, 1 mM EDTA, pH 7.5, 10 mM Na_2HPO_4, pH 7.4, 10 mM PMSF, 25 mM benzamidine, 1 mM leupeptin, 0.025 units/ml aprotinin). Equal amounts (80 µg) of cell proteins were separated by SDS-PAGE. The proteins on the gels were electro-transferred to nitrocellulose and reacted with the different MAbs. The bands derived form western blotting were scanned with a laser scanner (Epson 1260) and their intensities were quantified with Image J software (NIH).

AKT kinase assay

KB cells were treated with different concentrations VIP or VIP-DAP3 as described above. At the time of processing, 1 ml ice-cold cell lysis buffer (20 mM TRIS, pH 7.5, 150 mM NaCl, 1 mM EDTA, 1 mM EGTA, 1% Triton X-100, 2.5 mM sodium phosphate, 1 mM β-glycerophosphate, 1 mM sodium orthovanadate, 1 mg/ml leupeptin, 1 mM PMSF) was added to cells that were scraped and incubated on ice for 10 min. The cells were collected and transferred to microcentrifuge tubes and centrifuged at 1,200*g* for 10 min at 4°C. The supernatants were collected and precipitated, and were immobilized with 20 µl of Akt (IG1) monoclonal antibody crosslinked to agarose beads (Cell Signalling Technology, MA, USA) by o/n incubation

with gentle rocking at 4°C. The resulting immunoprecipitates were then incubated for 30 min at 30°C with 1 μg GSK-3 fusion protein (Cell Signalling Technology) in the presence of 200 mM ATP and kinase buffer (25 mM TRIS, pH 7.5, 5 mM β-glycerophosphate, 2 mM dithiothreitol, 0.1 mM sodium orthovanadate, 10 mM $MgCl_2$). The reaction was terminated with the addition of 20 μl 3× SDS sample buffer. The supernatants were boiled for 5 min and electrophoresed by 12% SDS-PAGE and the protein was electro-transferred on a nitrocellulose film. Phosphorylation of GSK-3 was detected using a probe anti-Phospho-GSK-3α/β(Ser21/9) rabbit polyclonal antibody (diluted 1:1,000) and then with a secondary anti-rabbit HRP-conjugated monoclonal antibody (diluted 1:2,000). The film was washed with TBS 1× 0.05% Tween 20 buffer and the specific reactivity was detected by chemiluminescence technique (Amersham).

Flow cytometry analysis of cell cycle

The KB and H1355 cells were seeded in 100 mm plates at the density of 1×10^6 cells/plate. After 12 and 24 h of incubation with VIP or VIP-DAP3 at 37°C, as described above, the cells were washed in PBS, pelleted in centrifuge and directly stained with a PI solution (50 μg PI in 0.1% sodium citrate, 0.1% NP40, pH 7.4) for 30 min at 4°C in the dark. Flow cytometric analysis was performed using a FACScan flow cytometer (Becton-Dickinson, San Jose, CA, USA). To evaluate cell-cycle PI, fluorescence was collected as FL2-H (linear scale) by the CellQuest software (Becton-Dickinson). For the evaluation of intracellular DNA content, at least 20,000 events for each point were analysed by CellQuest software in at least three different experiments giving a SD less than 5%.

Flow cytometric analysis of oxidative stress

The KB and H1355 cells were seeded in six-multiwell plates at the density of 3×10^5 cells/well. After 24-h incubation at 37°C, the cells were treated for 12 h with 250 μM H_2O_2 and/or VIP and VIP-DAP3. The H_2O_2 stress was analysed by hydroethidine (HE) staining. Hydroethidine, the sodium borohydride-reduced derivative of ethidium bromide (EB), which easily permeates cell membranes, is an oxygen radical-sensitive fluorescent probe. The intracellular hydroethidine can be directly oxidized to form red fluorescent EB, which in turn is trapped in the nucleus by intercalation into DNA hydroethidine is especially sensitive to superoxide anion and to a lesser degree to H_2O_2. The cells were incubated for 1 h after the end of treatment with 20 ng/ml hydroethidine stock solution (2.5 mg/ml). At the time of processing, the cells were scraped, washed twice with PBS and the pellet was resuspended in 1 ml PBS. The red fluorescent EB accumulation was analysed by FACScan flow cytometer (FACScan, Becton-Dickinson) by the CellQuest software. For each sample, 2×10^4 events were acquired. The analysis was carried out by triplicate determination on at least three separate experiments.

Intracellular lipid peroxidation (TBARs assay)

The lipid-peroxidation state was evaluated using an analytical-quantitative methodology. It predicts the formation of coloured adduct produced by the stoichiometric reaction of malondialdehyde (MDA) with TBA. The TBA–TCA solution was prepared dissolving 0.37 g of TBA in 100 ml of 15% trichloroacetic acid (TCA) in HCl 0.25 N and butylated hydroxytoluene BHT (7.2%) was dissolved in 98% ethanol. TBA reactive substances (TBARs) were measured on homogenate obtained by lysing 1×10^6 cells with 10% ice-cold TCA after incubation with VIP and VIP-DAP3 (10^{-10} and 10^{-11} M) for 12 and 24 h. The lysis mixture was centrifuged at 800*g* for 10 min. The assay was conducted incubating aliquots (1 ml) of supernatant and 2 ml of 0.37% TBA–15% TCA solution at 100°C for 30 min. The reaction was stopped putting the samples in cold water and after a centrifugation at 15,000*g* for 10 min the chromogen (TBARS) was quantified by Jenway Genova spectrophotometric reading at a wavelength of 532 nm. The concentration of MDA was determined by comparison with a standard reference curve according to Graber et al.

Statistical analysis

All data are expressed as mean ± SD. Statistical analysis was performed by analysis of variance (ANOVA) with Neumann–Keul's multiple comparison test or Kolmogorov–Smirnov where appropriate. The asterisks in the figure indicate significant difference between the cells treated with VIP-DAP3 respect to the cells treated with VIP (**$p < 0.003$, *$p < 0.05$, n.s. not significant).

Results

VIP and VIP-DAP3 effects on cell growth inhibition and cell-cycle perturbations induced by H_2O_2

The oxidative status of cells can modulate several cell functions and can be involved in physiological and pathological conditions. H_2O_2 has been frequently used for the induction of oxidative stress in vitro. We have evaluated the counteracting effects of VIP and VIP-DAP3 on the growth inhibition and S-phase reduction

caused by 250 μM H_2O_2 on both human head and neck cancer KB and NSCLC H1355 cell lines. H_2O_2 induced an about 20% growth inhibition after 24 h on both cell lines (Fig. 1a, b). VIP and VIP-DAP3 alone induced a time-dependent cell proliferation in both cell lines (Fig. 1a, b). In detail, VIP at the concentration of 10^{-11} M caused an about 20 and 15% increase of cell proliferation in KB and H1355 cells, respectively (Fig. 1a, b). Equimolar concentrations of VIP-DAP3 caused an about 35 and 20% increase of cell proliferation of KB and H1355 cells, respectively. Moreover, VIP addition to H_2O_2-treated cells antagonized the growth inhibition found in H1355 cells and indeed induced a 10% growth in KB cells. On the other hand, the addition of equimolar concentration of VIP-DAP3 indeed induced an about 25 and 20% growth stimulation in KB and H1355 cells, respectively (Fig. 1a, b). H_2O_2 reduced both KB and H1355 cell distribution in S-phase of the cell cycle (2 and 5%, respectively) as compared to untreated cells (6 and 13%, respectively) (Fig. 1c, d). On the other hand, KB and H1355 cells treated with 10^{-11} M VIP alone slightly accumulated in S-phase (10 and 14%, respectively), while the effect of equimolar concentration of VIP-DAP3 was more potent. In fact, the latter induced an about 12 and 22% S-phase accumulation in KB and H1355 cells, respectively (Fig. 1c, d). The addition of VIP to H_2O_2-treated cells partially antagonized the effects of H_2O_2 on H1355 and completely restored the distribution in S-phase on H1355 cells (Fig. 1c, d). On the other hand, the exposure of H_2O_2-treated cells to equimolar concentrations of VIP-DAP3 caused an increase of S-phase accumulation similar to that one induced by VIP-DAP3 alone (Fig. 1c, d). These data suggest that VIP-DAP3 is more potent than the native protein in antagonizing the effects induced by H_2O_2 on both cell proliferation and S-phase accumulation.

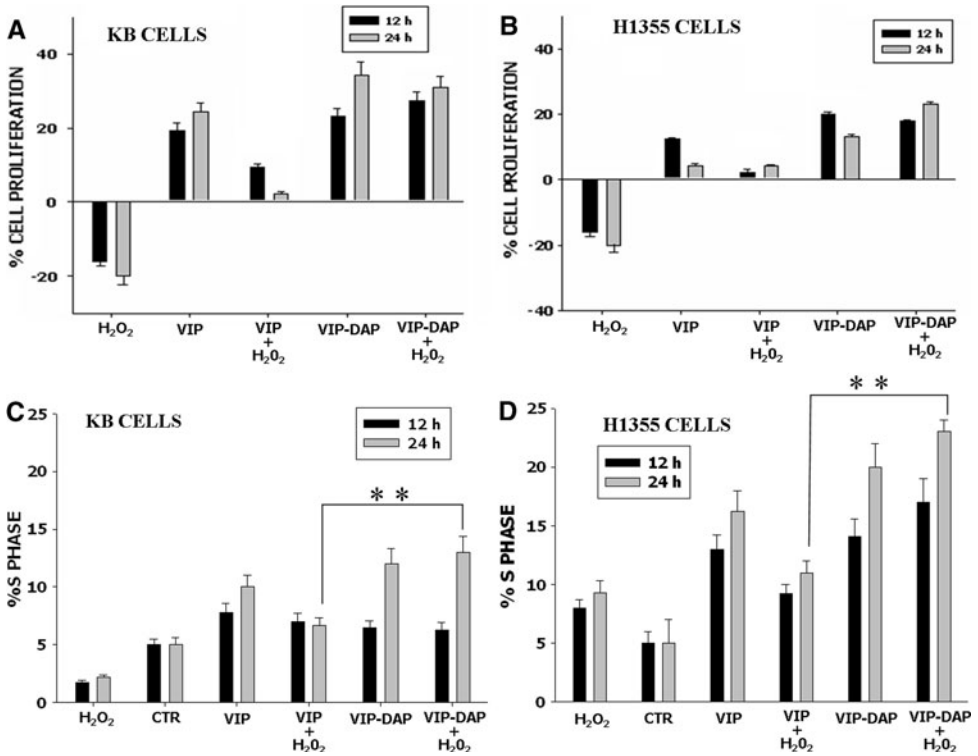

Fig. 1 VIP-DAP3 was more potent than VIP in antagonizing the effects of H_2O_2 on both proliferation and S-phase accumulation in human epithelial cancer cells. KB and H1355 cells were seeded and treated in the absence or presence of either 10^{-11} M VIP or 10^{-11} M VIP-DAP3 and/or 250 μM H_2O_2 at different exposure times. % proliferation induced by the different treatments after 12 and 24 h in KB (**a**) and in H1355 (**b**) epidermoid cancer cells evaluated with haemocytometric cell count. Each point is the mean of at least four different replicate experiments. *Bars* standard errors (SEs). After the same treatments, KB (**c**) and H1355 (**d**) cancer cells were fixed in methanol, labelled with PI and analysed at FACS for cell-cycle evaluation as described in "Materials and methods". The experiments were performed at least three times and the results were always similar. *CTR* control cells, *VIP* 10^{-11} M VIP, *VIP-DAP3* 10^{-11} M VIP-DAP3, H_2O_2 250 μM H_2O_2, *VIP* + H_2O_2 10^{-11} M VIP + 250 μM H_2O_2, *VIP-DAP3* + H_2O_2 10^{-11} M VIP-DAP3 + 250 μM H_2O_2. The *bars* represent mean ± SD of three independent experiments. *Asterisks* indicate significant difference between the cells treated with VIP-DAP3 respect to the cells treated with VIP. $^{**}p < 0.003$, $^{*}p < 0.05$

VIP and VIP-DAP3 effects on intracellular ROS increase induced by H_2O_2

We have evaluated the possible protective role of VIP and VIP-DAP3 on intracellular ROS increase induced by 12 h 250 μM H_2O_2 on KB and H1355 cells at FACS analysis after labelling with hydroethidine, a redox-sensitive probe. H_2O_2 caused an about 40% increase of intracellular ROS on both KB and H1355 cells as demonstrated by the evaluation of mean fluorescence intensity at FACS (Fig. 2a–c). 10^{-11} M VIP alone induced a 10 and 40% decrease of intracellular ROS in KB and H1355 cells, respectively (Fig. 2a, c); 10^{-11} M VIP-DAP3 caused a 20 and 50% reduction of intracellular ROS in KB and H1355 cells, respectively (Fig. 2b, c). The addition of VIP to H_2O_2-treated cells only partially antagonized the ROS increase determining a 20% increase of intracellular ROS on both cell lines. On the other hand, the addition of VIP-DAP3 to H_2O_2-treated cells completely antagonized the effects of H_2O_2 on ROS inducing indeed an about 10 and 20% reduction of the latter if compared to untreated counterparts in KB and H1355 cells, respectively (Fig. 2a–c). These data suggest that VIP-DAP3 is more potent than VIP in antagonizing the increase of ROS production induced by H_2O_2.

VIP and VIP-DAP3 effects on lipid peroxidation induced by H_2O_2

We have evaluated in KB cells, at the same experimental conditions, the peroxidation of membrane lipids as a marker of membrane damage induced by oxidative stress. The treatment of the cells for 12 and 24 h with H_2O_2 induced an about 200% increase of lipid peroxidation while 10^{-11} M VIP had no effects and VIP-DAP3 induced an about 120% decrease of lipid peroxidation in the same experimental conditions (Fig. 3). VIP only partially antagonized the effects of H_2O_2 on lipid peroxidation while

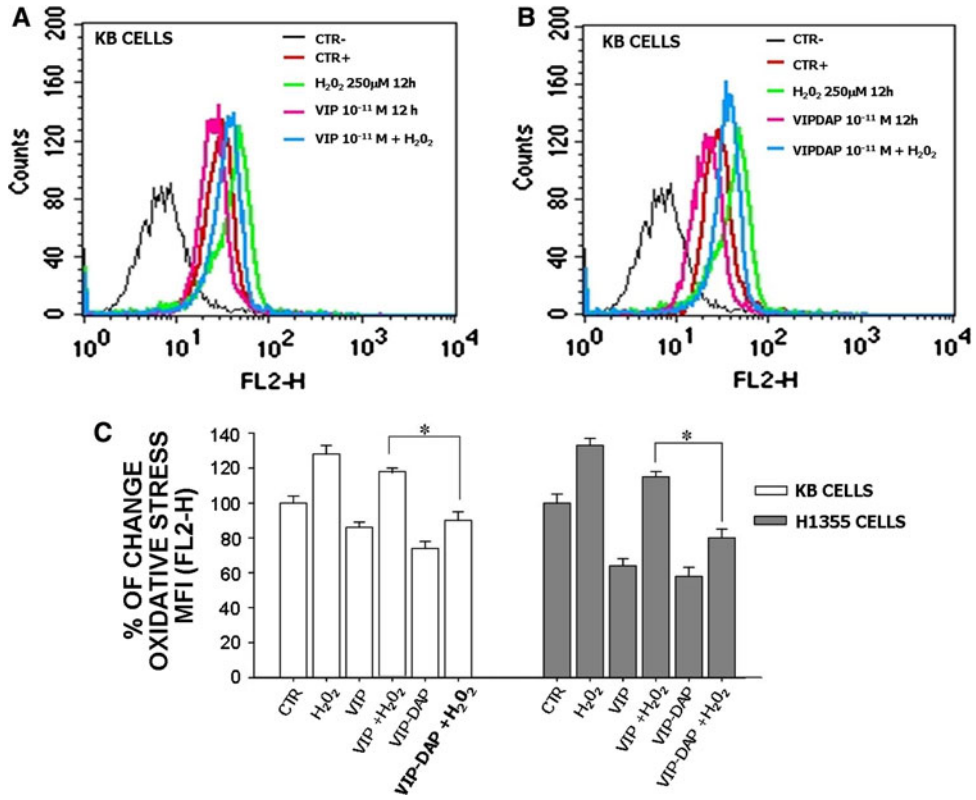

Fig. 2 VIP and VIP-DAP3 reduced the oxidative stress induced by H_2O_2. Flow cytometric analysis of oxidative stress in KB cells labelled with hydroethidine (HE) probe for measurement of intracellular O_2^- after either VIP (**a**) or VIP-DAP3 (**b**) alone or in combination with H_2O_2 treatment for 12 h. **a** *CTR*− HE-unlabelled cells, *CTR*+ HE-labelled cells, *H_2O_2* 250 μM H_2O_2, *VIP* 10^{-11} M VIP, *VIP/H_2O_2* 10^{-11} M VIP + 250 μM H_2O_2. **b** *CTR*− HE-unlabelled cells, *CTR*+ HE-labelled cells, *VIP-DAP* 10^{-11} M VIP-DAP3, *VIP* 10^{-11} M VIP, *VIP-DAP/H_2O_2* 10^{-11} M VIP-DAP3 + 250 μM H_2O_2. **c** *Columns* show mean fluorescence intensity (MFI) associated to the above histograms in the different experimental conditions in KB and H1355 cancer cells. The experiments were performed at least three different times and the results were always similar. The *bars* represent mean ± SD of three independent experiments. $^{**}p < 0.003$, $^{*}p < 0.05$

VIP-DAP3 caused a total restoration suggesting again an anti-oxidative activity stronger than that of native peptide (Fig. 3).

Inhibition of oxidative-stress pathway by VIP-DAP3

On the bases of these data, we have studied the effects of intracellular ROS on the activity and expression of the components of stress-activated signal transduction pathways and the ability of VIP and VIP-DAP3 in the counteraction of these effects. We have firstly evaluated the effects of VIP or VIP-DAP3 addition to H_2O_2 on the phosphorylation and expression of the stress-induced kinase p38 MAPK in KB cells by western blotting (Fig. 4a, b, f). We have found that 24 h H_2O_2 caused an about 50% increase of the activation ratio of p38 MAPK (the activation ratio was calculated making the ratio between the arbitrary intensities of the bands associated to phosphorylated p38 MAPK and that of the total p38 MAPK). The exposure of KB cells to 10^{-11} M VIP-DAP3, after 24 h, induced a 50% reduction of the p38 MAPK activation ratio while equimolar concentrations of VIP had no effects (Fig. 4a, b, f). KB cells treated with VIP and H_2O_2 had a 20% increase of p38 MAPK activation ratio that was, on the other hand, completely antagonized by VIP-DAP3 (an about 20% reduction of p38 MAPK activation ratio was recorded in these experimental conditions). Similarly, H_2O_2 caused an about 40% increase of HSP-70 expression while VIP had no effects and VIP-DAP3 induced an about 50% reduction of HSP-70 expression (Fig. 4c, f). VIP completely antagonized the effects induced by H_2O_2 while VIP-DAP3 caused indeed an about 30% reduction of HSP-70 expression (Fig. 4c, f). Moreover, H_2O_2 caused an about 40% increase of HSP-27 expression while VIP had no effects and VIP-DAP3 induced an about 50% reduction of HSP-27 expression (Fig. 4d, f). In this case, VIP was not able to antagonize the effect induced by H_2O_2 recording indeed a 100% increase of HSP-27 expression. On the

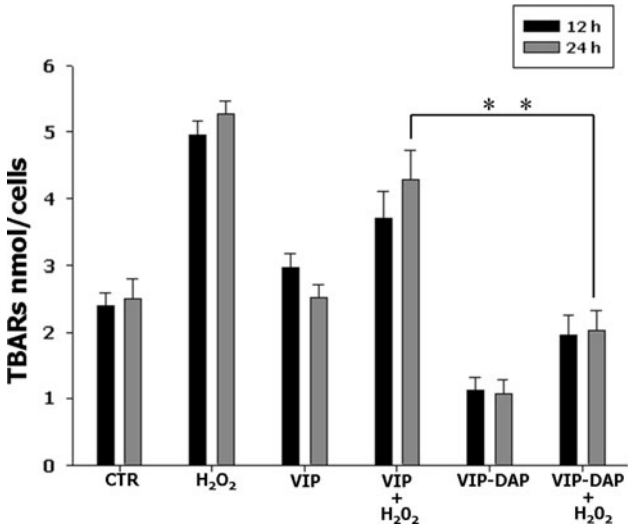

Fig. 3 Effects of VIP and VIP-DAP3 on lipoperoxidation induced by oxidative stress in KB cells. The grade of lipid membrane peroxidation was evaluated in KB cells through changes of malondialdehyde (MDA) levels expressed as % of thiobarbituric acid reactive substances (TBARs), as described in "Materials and methods". Cells were incubated for 12 or 24 h with either VIP or VIP-DAP3 in the absence or presence of H_2O_2. The experiments were performed at least three different times and the results were always similar. *Bars* standard deviations (SDs). *CTR* untreated KB cells, *H_2O_2* 12 h 250 μM H_2O_2, *VIP* 10^{-11} M 12 h VIP, *VIP/H_2O_2* 12 h 10^{-11} M VIP + 250 μM H_2O_2, *VIP-DAP* 10^{-11} M VIP-DAP3, *VIP* 10^{-11} M 12 h VIP, *VIP-DAP/H_2O_2* 12 h 10^{-11} M VIP-DAP3 + 250 μM H_2O_2. The *bars* represent mean ± SD of three independent experiments. $^{**}p < 0.003$, $^{*}p < 0.05$

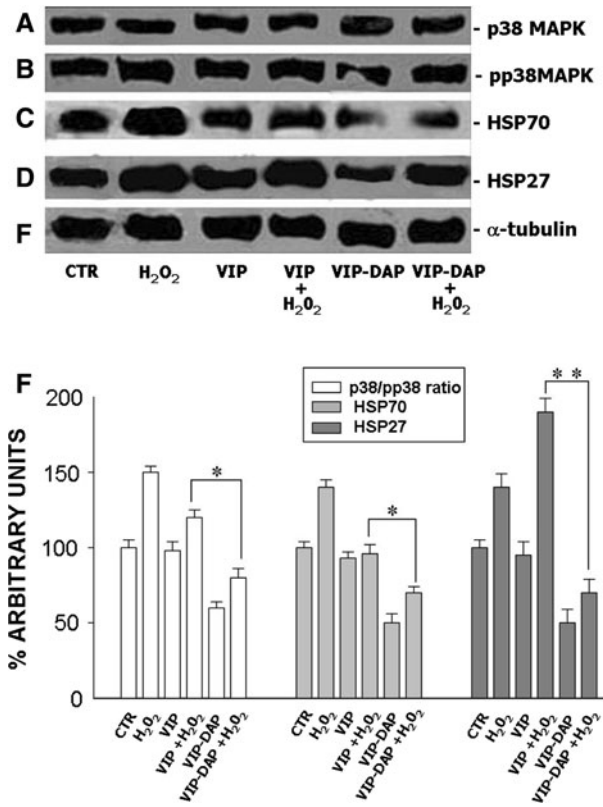

Fig. 4 Effects of VIP and VIP-DAP3 on stress-activated signal transduction pathways induced by H_2O_2. Western blot assay for the expression (**a**) and phosphorylation (**b**) of p38 kinase evaluated after blotting with an anti-p38 and an anti-pp38 specific antibodies, respectively, as described in "Materials and methods". Determination of the expression of the HSP-70 (**c**) and HSP-27 (**d**) evaluated after blotting with specific antibodies as described in "Materials and methods". **e** Expression of the house-keeping protein α-tubulin, used as loading control. **f** Laser scanner of the bands associated to proteins. The intensities of the bands were expressed as % arbitrary units. *Bars* SEs. The experiments were performed at least three different times and the results were always similar. *CTR* untreated KB cells, *H_2O_2* 250 μM H_2O_2, *VIP* 10^{-11} M VIP, *VIP/H_2O_2* 10^{-11} M VIP + 250 μM H_2O_2, *VIP-DAP* 10^{-11} M VIP-DAP3, *VIP* 10^{-11} M VIP, *VIP-DAP/H_2O_2* 10^{-11} M VIP-DAP3 + 250 μM H_2O_2. $^{**}p < 0.003$, $^{*}p < 0.05$

other hand, a 30% reduction of HSP-27 expression was observed in KB cells treated at the same time with VIP-DAP3 and H_2O_2 (Fig. 4d, f). In conclusion, VIP-DAP3 is again a stronger inhibitor of the oxidative stress-mediated signal transduction pathway in KB cells.

Effects of VIP and VIP-DAP3 on the modulation of Erk and Akt enzyme activity by oxidative stress

The Erk and Akt pathways are well-known survival and proliferative pathways of human epidermoid cells. Therefore, we have evaluated both Akt and Erk activity after exposure of KB cells to H_2O_2 and in the presence or absence of either VIP or VIP-DAP3. The addition of H_2O_2 to KB cells for 24 h induced an about 40 and 60% reduction of both Erk-1/2 and Akt activity, respectively (Fig. 5b, d). On the other hand, no changes of the expression of the two kinases were found in the same experimental conditions (Fig. 5a, c). We have found that 24-h incubation of KB cells with VIP at the concentration of 10^{-11} M did not induce significant changes of both the activity and the expression of the two kinases while equimolar concentrations of VIP-DAP3 caused an about 40 and 30% increase of the activity of both Erk-1/2 and Akt, respectively (Fig. 5). VIP was able to totally antagonize the effects of the oxidative stress on Erk-1/2 activity but only partially abrogated the reduction of Akt activity caused by H_2O_2 (in fact, an about 40% reduction of Akt activity was still recorded in these experimental conditions) (Fig. 5). On the other hand, the treatment of KB cells for 24 h with VIP-DAP3 and H_2O_2 caused an about 60% increase of Erk-1/2 activity and completely antagonized the effects induced by oxidative stress on Akt activity (Fig. 5). Therefore, the antagonism induced by VIP-DAP3 on the oxidative stress-activated signal transduction pathways was paralleled by an increase of the activity of proliferative and survival pathways in KB cells.

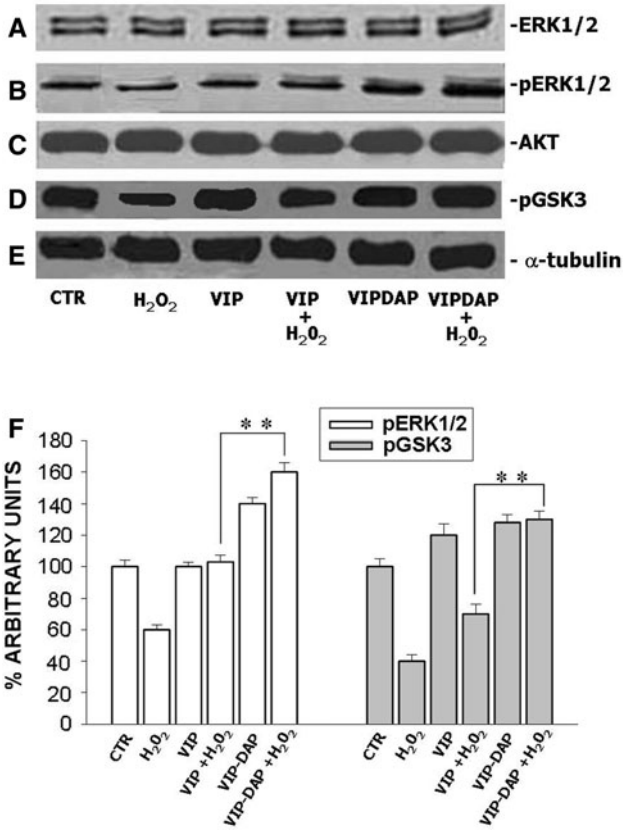

Fig. 5 Effects of VIP and VIP-DAP3 on the changes induced by oxidative stress on Erk and AKT survival pathways. Western blot assay for the expression (**a**) and phosphorylation (**b**) of Erk-1 and -2 evaluated with an anti-MAPK and an anti-pMAPK specific Mab, respectively, as described in "Materials and methods". Determination of the AKT expression by western blotting (**c**). **d** Precipitation of AKT with anti-Akt monoclonal antibody immobilized with agarose beads and incubation with GSK3 for the evaluation of AKT activity. The phosphorylation of GSK-3 was detected using a probe anti-Phospho-GSK polyclonal as described in "Materials and methods". **e** Expression of the house-keeping protein α-tubulin, used as loading control. **f** Laser scanner of the bands associated to proteins. The intensities of the bands were expressed as % arbitrary units. The experiments were performed at least three different times and the results were always similar. *CTR* untreated KB cells, H_2O_2 250 μM H_2O_2, *VIP* 10^{-11} M VIP, *VIP/H*$_2$*O*$_2$ 10^{-11} M VIP + 250 μM H_2O_2, *VIP-DAP* 10^{-11} M VIP-DAP3, *VIP* 10^{-11} M VIP, *VIP-DAP/H*$_2$*O*$_2$ 10^{-11} M VIP-DAP3 + 250 μM H_2O_2. $^{**}p < 0.003$, $^{*}p < 0.05$

Discussion

The potential use of VIP in the treatment of important chronic diseases (such as infections, asthma, rheumatoid arthritis, sarcoidosis, connective tissue disorders, etc.) has stimulated a variety of studies investigating the relationships between structure and molecular mechanisms of action of this potential drug. Structural activity studies, performed on a number of analogous and different VIP fragments, demonstrated that full action of VIP is critically dependent of the integrity of the moiety. In a previous paper published by our group, an interdisciplinary approach of molecular modelling and computational chemistry for the characterization of the structure–activity features of VIP in order to increase its therapeutic index in human diseases was reported. Our data suggested that the introduction of a positive charge (DAP group) at the level of Gln16 of VIP by TGase reaction increases both its biological functions (cell-cycle modulation and anti-oxidative activity) and its stability to proteolysis (De Maria et al. 2002; Caraglia et al. 2006; Caraglia et al. 2008). In the present report, we show the effects of VIP and VIP-DAP3 on human oropharyngeal epidermoid carcinoma KB and lung epidermoid carcinoma H1355 cell lines following oxidative stress induced by H_2O_2. The choice of the experimental model was due to both the ability of these

cells to grow in vitro and to the reported expression of VIP receptors (data not shown).

Oxidative stress is a common associative mechanism that is part of the pathogenesis of several degenerative disorders. VIP is a neuropeptide involved in the normal development and in the protection from ageing derived from its protective effects against oxidative stress. It is widely reported that cells treated with H_2O_2 are growth inhibited and the addition of VIP is able to antagonize this effect (Saga and Said 1984). Therefore, in the present study, we have compared the VIP and VIP-DAP3 effects on oxidative stress-induced cell growth inhibition and signal transduction activity in KB and H1355 cells. We have found, as expected, that H_2O_2 inhibited cell proliferation and VIP-DAP3, more than VIP, induced a time- and dose-dependent antagonistic effect on both cell growth inhibition and reduction of % of cells in S-phase of the cell cycle. In detail, VIP was only able to restore the proliferation and S-phase accumulation while VIP-DAP3, at the same times and concentrations, indeed induced an increase of the proliferative status of both KB ad H1355 cells. These effects were paralleled by a strong antagonism induced by VIP-DAP3 on the increase of intracellular ROS and on the peroxidation on cellular phospholipids caused by H_2O_2 on both KB and H1355 cells. Again the effect of VIP-DAP3 was stronger than that caused by VIP.

Delgado has recently demonstrated that VIP acts inhibiting ROS-induced phosphorylation of stress-activated protein kinases SAPK/JNK and p38 MAPK. In fact, VIP inhibits MEKK1 activity and the subsequent phosphorylations of MEK4, JNK, and c-Jun (Delgado 2002). The VIP interference with the stress-induced SAPK/JNK pathway may represent a significant element in the regulation of inflammatory response (Groneberg et al. 2001). In our study, we have showed that VIP-DAP3 reduces in KB cells not only the expression and phosphorylation of p38 kinase but also the expression of both HSP-70 and -27, other mediators of stress. Interestingly, VIP was again less potent than VIP-DAP3 and was not able to antagonize the effects of oxidative stress on HSP-27 that was indeed 100% increased in the combined treatment.

Pituitary adenylate cyclase-activating polypeptides (PACAP-27 and -38) are neuropeptides of the VIP/secretin/glucagon family. Studies on the effect of PACAP-38 on apoptosis induced by potassium deprivation in cerebellar neuron cells have demonstrated that PACAP-38 increased survival in a dose-dependent manner decreasing the extent of apoptosis. PACAP-38 induced activation of the Erk-type MAP kinases. PD98059, an inhibitor of MEK (MAP kinase kinase), completely abolished the anti-apoptotic effect of PACAP-38, suggesting that MAP kinase pathway activation is necessary for PACAP-38 effect (Journot et al. 1998). In our experimental model, we have found that VIP-DAP3, in the presence of H_2O_2, increased the activation of both Erk-1 and 2 without changes in their total protein expression. These results are in agreement with the previous report on PACAP-38.

Thereafter, we have evaluated the effects of VIP and VIP-DAP3 on another important survival pathway regulated by ras, the Akt/PKB signalling. In detail, we have studied both Akt expression and activity with western blotting and in gel kinase assay, respectively. We have found that only VIP-DAP3 increased Akt activity, also in the presence of H_2O_2, while VIP, at the same concentration, was not able to completely antagonize the effects of oxidative stress on Akt activity.

In conclusion, in vitro VIP-DAP3 appears to be more active than VIP, indicating that the stabilized structure of the peptide increases protective effect from oxidative stress potentiating both survival and cell proliferation of epidermoid cancer cells.

References

Cameron AR, Johnston CF, Kirkpatrick CT, Kirkpatrick MC (1983) The quest for the inhibitory neurotransmitter in bovine tracheal smooth muscle. J Exp Physiol 68:413–426

Caraglia M, Dicitore A, Giuberti G, Cassese D, Lepretti M, Cartenì M, Abbruzzese A, Stiuso P (2006) Effects of VIP and VIP-DAP on proliferation and lipid peroxidation metabolism in human KB cells. Ann N Y Acad Sci 1070:167–172

Caraglia M, Carteni M, Dicitore A, Cassese D, De Maria S, Ferranti P, Giuberti G, Abbruzzese A, Stiuso P (2008) Experimental study on vasoactive intestinal peptide (VIP) and its diaminopropane bound (VIP-DAP) analog in solution. Amino Acids 35(2):275–281

Coles SJ, Said SI, Reid ML (1981) Inhibition by vasoactive intestinal peptide of glycoconjugate and lysozyme secretion by human airways in vitro. Am Rev Respir Dis 124:531–536

Cooke HJ (2000) Neurotransmitters in neuronal reflexes regulating intestinal secretion. Ann N Y Acad Sci 915:77–80

De Maria S, Metafora S, Metafora V, Morelli F, Robberecht P, Waelbroeck M, Stiuso P, De Rosa A, Cozzolino A, Esposito C, Facchiano A, Cartenì M (2002) Transglutaminase-mediated polyamination of vasoactive intestinal peptide (VIP) Gln16 residue modulates VIP/PACAP receptor activity. Eur J Biochem 269:3211–3219

Delgado M (2002) Vasoactive intestinal peptide and pituitary adenylate cyclase-activating polypeptide inhibit the MEKK1/MEK4/JNK signaling pathway in endotoxin-activated microglia. Biochem Biophys Res Commun 293(2):771–776

Delgado M, Abad C, Martinez C, Juarranz MG, Arranz A, Gomariz RP, Leceta J (2002) Vasoactive intestinal peptide in the immune system: potential therapeutic role in inflammatory and autoimmune diseases. J Mol Med 80:16–24

Gourlet P, Vilardaga JP, De Neef P, Waelbroeck M, Vandermeers A, Robberecht P (1996) The C-terminus ends of secretin and VIP interact with the N-terminal domains of their receptors. Peptides 17:825–829

Groneberg DA, Springer J, Fischer A (2001) Vasoactive intestinal polypeptide as mediator of asthma. Pulm Pharmacol Ther 14:391–401

Holtmann MH, Hadac EM, Miller L (1995) Critical contributions of amino-terminal extracellular domains in agonist binding and activation of secretin and vasoactive intestinal polypeptide receptors. Studies of chimeric receptors. J Biol Chem 270(24):14394–14398

Inanami O, Ohta T, Ito S, Kuwabara M (1999) Elevation of intracellular calcium ions is essential for the H_2O_2-induced activation of SAPK/JNK but not for that of p38 and ERK in Chinese hamster V79 cells. Antiox Redox Signal 1:501–508

Ishioka C, Yoshida A, Kimata H, Mikawa H (1992) Vasoactive intestinal peptide stimulates immunoglobulin production and growth of human B cells. Clin Exp Immunol 87:504–508

Journot L, Villalba M, Bockaert J (1998) PACAP-38 protects cerebellar granule cells from apoptosis. Ann N Y Acad Sci 11865:100–110

Koh SW, Waschek JA (2000) Corneal endothelial cell survival in organ cultures under acute oxidative stress: effect of VIP. Invest Ophthalmol Vis Sci 41:4085–4092

Kuwabara M, Asanuma T, Niwa K, Inanami O (2008) Regulation of cell survival and death signals induced by oxidative stress. J Clin Biochem Nutr 43(2):51–57

Martin SC, Shuttleworth TJ (1996) The control of fluid-secreting epithelia by VIP. Ann N Y Acad Sci 805:133–147

Matsuzaki Y, Hamasaki Y, Said SI (1980) Vasoactive intestinal peptide: a possible transmitter of nonadrenergic relaxation of guinea pig airways. Science 210:1252–1253

Nicole P, Lins L, Rouyer-Fessard C, Drouot C, Fulcrand P, Thomas A, Couvineau A, Martinez J, Brasseur R, Laburthe M (2000) Identification of key residuesfor interaction of vasoactive intestinal peptide with human VPAC1 and VPAC2 receptors and development of a highly selective VPAC1 receptor agonist. Alanine scanning and molecular modeling of the peptide. J Biol Chem 275:24003–24012

Niwa K, Inanami O, Yamamori T, Ohta T, Hamasu T, Kuwabara M (2003) Redox regulation of PI3K/Akt and p53 in bovine endothelial cells exposed to hydrogen peroxide. Antiox Redox Signal 5:713–722

Nussdorfer GG, Bahcelioglu M, Neri G, Malendowicz LK (2000) Distribution, functional role, and signaling mechanism of adrenomedullin receptors in the rat adrenal gland. Peptides 21:309–324

Onoue S, Matsumoto A, Nagano Y, Ohshima K, Ohmori Y, Yamada S, Kimura R, Yajima T, Kashimoto K (2004) Alpha-helical structure in the C-terminus of vasoactive intestinal peptide: functional and structural consequences. Eur J Pharmacol 485:307–316

Saga T, Said SI (1984) Vasoactive intestinal peptide relaxes isolated strips of human bronchus, pulmonary artery, and lung parenchyma. Trans Assoc Am Phys 97:304–310

Said SI (1991) VIP as a modulator of lung inflammation and airway constriction. Am Rev Respir Dis 143:S22–S24

Sherwood NM, Krueckl SL, Mcrory JE (2000) The origin and function of the pituitary adenylate cyclase-activating polypeptide (PACAP)/glucagon superfamily. Endocr Rev 21(6):619–670

Shoge K, Mishima HK, Saitoh T, Ishihara K, Tamura Y, Shiomi H, Sasa M (1998) Protective effects of vasoactive intestinal peptide against delayed glutamate neurotoxicity in cultured retina. Brain Res 809:127–136

Sirangelo I, Iannuzzi C, Vilasi S, Irace G, Giuberti G, Misso G, D'Alessandro A, Abbruzzese A, Caraglia M (2009) W7FW14F apomyoglobin amyloid aggregates-mediated apoptosis is due to oxidative stress and Akt inactivation caused by Ras and Rac. J Cell Physiol 221(2):412–423

Tsuji M, Inanami O, Kuwabara M (2000) Neuroprotective effect of α-phenyl-*N*-*tert*-butylnitrone in gerbil hippocampus is mediated by the mitogen-activated protein kinase pathway and heat shock proteins. Neurosci Lett 282:41–44

Xia Z, Dickens M, Raingeaud J, Davis RJ, Greenberg ME (1995) Opposing effects of ERK and JNK-p38 MAP kinases on apoptosis. Science 270:1326–1331